Measurement of the Interfacial Attraction Between Graphene Oxide Sheets and the Polymer in a Nanocomposite

D. E. Kranbuehl,[1,2] M. Cai,[1] A. J. Glover,[1,2] H. C. Schniepp[1]

[1]*Department of Applied Science, The College of William and Mary, Williamsburg, Virginia 23187*
[2]*Department of Chemistry, The College of William and Mary, Williamsburg, Virginia 23187*

Received 28 April 2011; accepted 28 April 2011
DOI 10.1002/app.34787
Published online 11 August 2011 in Wiley Online Library (wileyonlinelibrary.com).

ABSTRACT: The objective of this work was to characterize and, thereby, achieve a fundamental scientific understanding at the molecular level of the relationship of the intermolecular forces measured at the nanoscale between an individual nanoparticle and a polymer. In this study, we developed a method to directly characterize and measure the relative strength of the interfacial attractive forces between graphene oxide (GO) nanoparticles and the polymer matrix on the nanoscale using atomic force microscopy techniques to evaluate individual particles. The method was successfully applied to study the interfacial attractive forces in GO–polymer nanocomposites. Two polymers [poly(methyl methacrylate) and poly(vinyl alcohol)] were studied. The results support that this method is capable of characterizing the interfacial attractive forces directly at the nanoscale. The method can be applied to other nanoparticle–macromolecular systems, allowing the determination of the interaction strength between nanoparticles and the macromolecular material. This information paves the way to characterize the relationship between interfacial forces at the nanometer level to a nanocomposite's performance properties. © 2011 Wiley Periodicals, Inc. J Appl Polym Sci 122: 3740–3744, 2011

Key words: atomic force microscopy (AFM); interfaces; nanocomposites

INTRODUCTION

Polymer nanocomposite materials, which contain nanoparticles embedded in polymers, have advanced properties and great potential to be multifunctional, high-performance, lightweight materials.[1–3] Graphene, the single atomic plane of graphite, has outstanding mechanical, electrical, and barrier properties.[4,5,6] Monolayer graphene has a Young's modulus as high as 1.0 TPa,[7] which makes it a promising reinforcing phase for ultrastrong structural composite materials.[8] However, graphene nanoparticles are highly hydrophobic and are thus extremely difficult to disperse in solvents.[9,10] This limits the application of pure graphene sheets in nanocomposites. Functionalized graphene sheets,[11–16] which have functional side groups, such as epoxy (C—O—C) and hydroxyl (C—OH) groups, attached to the carbon backbone surface,[17] are compatible with a wider variety of solvents. Moreover, large-scale production of single graphene sheets is possible and motivates the use of graphene as a reinforcing filler in advanced composites.[18–22] These nanocomposites have the potential for widespread applications as structural materials in aerospace, civil engineering, sports equipment, and biological implants because of the significant enhancement in the performance properties.

The mechanical properties of composites depend not only on the dispersion and mechanical properties of the nanofiller in the polymer but also very strongly on the properties of the polymer–particle interface. Thus, of major fundamental importance is the development of experimental methods to measure the intermolecular forces between an individual graphene nanoparticle and the polymer. The next fundamental scientific challenge is to understand the relationship between the particle–polymer interfacial forces measured at nanodimensions and the resulting macroscopic mechanical properties of the nanoparticle–polymer composite. In this study, we were particularly interested in graphene oxide (GO) with an atomic C:O ratio of 2 and its interfacial interaction with poly(vinyl alcohol) (PVA) and with poly(methyl methacrylate) (PMMA).

In this study, we developed a novel method to directly measure the relative attractive strength between two materials, the two-dimensional graphene sheets and the polymer in the nanocomposite, at the nanoscale using atomic force microscopy (AFM). In this method, the nanoparticle graphene sheets were sandwiched between two different

Correspondence to: H. C. Schniepp (schniepp@wm.edu).

materials possessing atomically smooth surfaces. After separation of these two materials, where we peeled off one material from the other, the graphene sheets were prone to stick on one of the surfaces. This depended on the difference in the interfacial attractive forces between the graphene sheets and these two materials. Thereby, we could compare the strength of the interfacial forces between the nanoparticle and the top surface of the polymer to the interfacial forces between the nanoparticle and the bottom substrate. In this manner, we could assess the relative strength of the GO nanoparticle with one substance compared to another. This provided the information we needed to vary the particle's surface chemistry, such as the carbon:oxygen ratio, and to optimize the interfacial attraction. Alternatively, one could use this method to select a polymer chemical structure that optimizes the interfacial attractive forces for a particular GO nanoparticle.

Here, this method is described and then used to characterize and understand the relative strength of the interfacial attractive forces between GO and PMMA and GO and PVA.

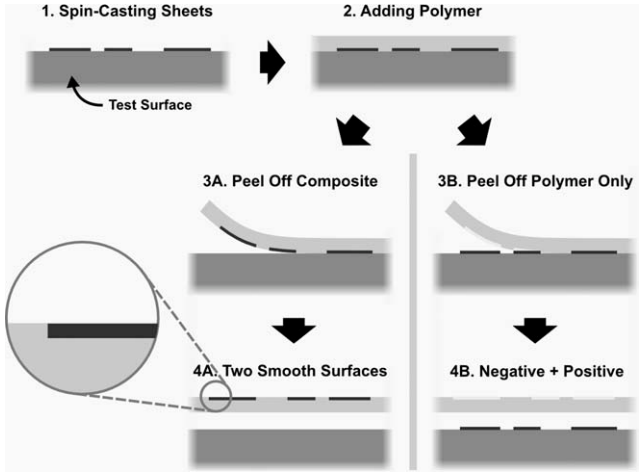

Figure 1 Illustration of the method to make nanocomposites with filler particles located at the composite surface. Two situations can be observed, each depending on the relative strength of the adhesion at the GO–polymer interface and the GO–substrate interface. For most polymer/substrate combinations, the sheets are either on the polymer (3A,4A) or on the substrate (3B,4B) surface after the peeling step (3).

EXPERIMENTAL

Preparation of GO

We made the GO filler sheets by first completely oxidizing graphite powder. The oxidization of graphite powder (Asbury Carbons, Asbury, NJ, grade 3243, 99.5%) was completed according to the Hummers method.[23] The dried graphite oxide flakes were exfoliated in deionized water or dimethylformamide (Acros, Morris Plains, NJ, extra dry, 99.8%) into individual graphene sheets by ultrasonication (Microson XL2007 tip sonicator with a power of 100 W, Microson, Farmingdale, NY). This produced a uniform and stable dispersion of single-layer GO sheets in solvents as verified by AFM that could stay uniform for several weeks without significant precipitation. Unlike with montmorillonite and carbon nanotubes, graphene sheets can be dispersed as individual nanoparticles in a polymer via solution processing. This is a very large advantage to these two widely studied systems.

The graphene sheets prepared by this method contained functional groups, such as epoxy and hydroxyl groups, attached to the hexagonal carbon backbone. The atomic carbon:oxygen ratio was determined to be 1.95 by Galbraith Laboratories (Knoxville, TN).

Preparation of the AFM samples

To study the interfacial forces between the graphene sheet and another material at the nanoscale, AFM (NT-MDT, NTEGRA Prima, Zelenograd, Russia) was ideally suitable. The AFM characterization of GO on traditional AFM substrates, mica, and highly oriented pyrolytic graphite (HOPG) has been reported.[15] Detecting the presence of GO on a polymer surface allowed us to examine the relative strength of the interfacial forces between GO and the polymer compared to mica, HOPG, and other polymers. AFM samples of GO on mica and HOPG were prepared by the spin-coating (WS-650SZ spin processor, Laurell Technologies Corp., North Wales, PA) of GO in a dimethylformamide dispersion with a concentration of 0.1 mg/mL onto freshly cleaved mica or HOPG.

To investigate GO on a polymer surface, the polymer surface had a roughness smaller than the thickness of the single-layer graphene sheets, that is, near atomic smoothness. A special procedure was applied to prepare these samples with atomically smooth surfaces. As described in Figure 1, GO was first spin-cast onto one material, the base material [see Fig. 1(1)]. We adopted mica and HOPG here because of their atomically smooth surfaces. Then, the polymer solution was added by drop-casting on top of the mica or HOPG [see Fig. 1(2)]. The samples were heated to evaporate the solvent. After solidification, the polymer film was peeled off from mica or HOPG [see Fig. 1(3A)]. In this way, the polymer surface in contact with mica or HOPG had sufficient surface smoothness for AFM examination. Then, this polymer film was mounted with the smooth surface facing up [see Fig. 1(4A)].

During AFM characterizations (Fig. 2), contact mode, tapping mode, and force modulation mode (FMM) were used. The tips were BudgetSensors

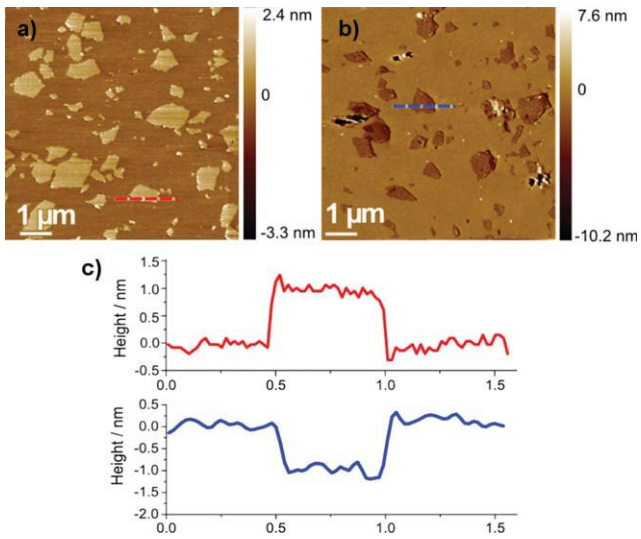

Figure 2 PMMA film peeled off from GO spin-coated on mica substrate: (a) AFM image of the mica substrate after peeling, showing positive topography. (b) AFM image of the PMMA surface, showing negative topography, which is shown to be the GO imprint. (c) The cross sections are shown in the (a) top line and (b) bottom line. [Color figure can be viewed in the online issue, which is available at wileyonlinelibrary.com.]

(Sofia, Bulgaria) SiNi triangular cantilevers with a force constant of 0.27 N/m, a radius of curvature of 15 nm, and a resonance frequency of 30 kHz. In FMM, a modulation signal with a frequency typically in the range of several kilohertz (less than the resonance frequency of the cantilever) was added to the voltage controlling the vertical position of the scanning piezo. The sample height was modulated vertically during scanning, whereas the tip was kept in contact on the surface with constant cantilever deflection. This led to a variation of the cantilever modulation amplitude, which depended on the sample local stiffness. On a soft material, the tip would indent deeper into the sample at the modulation frequency, inducing small tip modulation amplitude. In contrast, the tip modulation amplitude would be larger on a hard material. Thus, the magnitude of this amplitude indicated the local sample stiffness.[24,25]

RESULTS AND DISCUSSION

We used this newly developed peeling method to directly measure the relative interfacial attraction strength between the graphene nanosheets and two polymers, PVA and PMMA, on the length scale of the individual nanoparticles. The major steps in the method were described and are demonstrated in Figure 1. First, the GO nanosheets were spin-coated onto one material, which was called the base material. Then, a second material, the polymer, was spin-coated on top of the base material. In this way, the nanoparticle sheets of graphene were sandwiched between two different materials. By sandwiching the nanosheets, we constructed two interfaces: the base material–nanosheet interface and the polymer material–nanosheet interface. Next, we peeled off the polymer material from the base material, breaking one of the previous two interfaces. Then, AFM was used to examine both surfaces for the presence of nanosheets.

For the four materials tested here—PVA, PMMA, mica, and HOPG—we found that all of the sheets stuck only to one of the two materials. Consequently, two scenarios occurred because of differences in the interfacial attractive forces. If all the sheets stuck to the attached polymer material [see Fig. 1(3A,4A)], a featureless surface would have been found for the base material surface. At the same time, the surface of the attached material would have been found to be flat and contain graphene nanosheets embedded in the surface. This situation would imply that the polymer–nanoparticle interface had stronger attractive forces than the base material–nanoparticle interface. In the second scenario, all of the sheets would still be on the base material after peeling off the polymer. At the same time, this would leave the imprints on the peeled-off polymer [see Fig. 1(3B, 4B)]. When examining both surfaces, we should have found that the base material surface contained topographical features of single-layer graphene, whereas the peeled-off attached material would show a negative topography, which were the nanoscale imprints of the graphene (Figure 2). Therefore, this scenario implied that the interfacial attractive forces between the polymer material and the nanoparticles were weaker than between the graphene particles and the base material.

We applied this method to examine the interfacial attraction between graphene nanoparticles and the polymers PVA and PMMA relative to the attractive forces between graphene nanoparticles and the base materials, mica and HOPG. AFM contact mode was applied to display the surface topographies of the base material and the polymer material. When the graphene nanosheets were embedded within the polymer, the polymer surface should have been flat with a featureless topography, as Figure 1(4A) shows. In Figure 1(3B,4B), the case of contact-mode AFM only revealed the surface topography of the polymer and was unable to detect the presence of the graphene sheets. In this scenario, tapping mode or FMM were needed to detect the graphene embedded in the polymer surface. The phase in AFM tapping mode recorded the phase lag between the tip oscillation and the actuating signal during scanning and reflected the differences in the stiffness and the chemical compositions of components in the sample. The magnitude of the cantilever amplitude in FMM was sensitive to the sample stiffness and capable of mapping the local stiffness. Because of the large

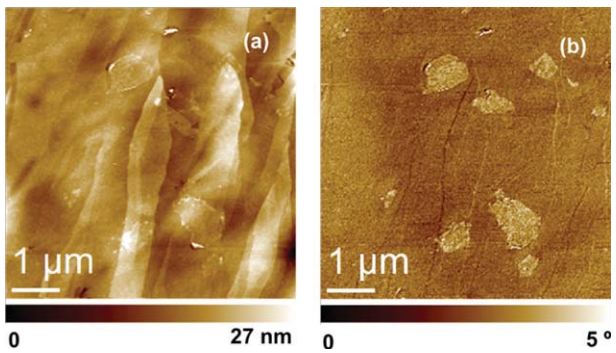

Figure 3 PMMA film peeled off from the HOPG substrate on which GO was spin-coated: (a) AFM tapping mode topography and (b) tapping-mode phase image. [Color figure can be viewed in the online issue, which is available at wileyonlinelibrary.com.]

discrepancy in the stiffness of the GO sheets and the surrounding polymers, the phase image in tapping mode and the amplitude image in FMM were able to easily reveal the sheets embedded in the polymer.

First, the interfacial attraction strength between GO and PMMA was examined with mica as the base material, GO as the sandwiched nanoparticle, and PMMA as the attached polymer material. The AFM contact-mode topography of the mica surface and the PMMA surface after peeling off are shown in Figure 2. Figure 2(a) shows that GO was still on the mica surface, giving the positive topography, and the PMMA surface displayed the corresponding imprints with negative topography, as shown in Figure 2(b). The height of GO on mica and the imprint on PMMA are given in Figure 2(c). It is notable that the thicknesses of both the positive and negative topography were around 1 nm; this corresponded to the thickness of single-layer GO. This further proved that the negative topography on the PMMA surface was induced by GO. To sum up, the case of PMMA peeling off from mica corresponded to scenario B described in Figure 1(3B,4B). Therefore, the PMMA–GO interface had weaker attractive forces than the mica–GO interface.

When the mica base material was replaced by HOPG, the result was the other scenario. The AFM tapping mode was conducted to scan the PMMA surface. The nanoparticles were buried in the topography of the PMMA surface [Fig. 3(a)]. The phase image of the AFM tapping mode clearly exhibited GO on the surface [Fig. 3(b)]. This implies that the GO nanoparticles were embedded into the PMMA surface; this made them undetectable in the contact mode topography but clearly visible in the phase image of the AFM tapping mode, which measured hardness. Moreover, no graphene sheets were found when we examined the HOPG surface. Therefore, this case was exactly the same as the scenario depicted by Figure 1(3A,4A) and revealed that the GO–PMMA interfacial attractive forces were stronger than the GO–HOPG interfacial forces.

This method was also applied to examine the interfacial forces between GO and PVA with mica as the base material and PVA as the polymer matrix. The results are shown in Figure 4. The PVA surface was relatively flat and smooth, as seen in Figure 4(a). The presence of GO in the polymer surface was, again, difficult to detect by contact mode. To detect the presence of GO, the AFM FMM was conducted on the PVA surface. The FMM image of the PVA surface is shown in Figure 4(b). Because GO sheets were much stiffer than the surrounding PVA, they were able to induce much bigger changes in the cantilever amplitude in FMM and, thus, produce brighter spots in the FMM image. In Figure 4(b), brighter features were detected on the surface, which indicated the presence of GO. The graphene sheets were actually embedded within the PVA; this made them undetectable in the topography using the tapping mode or the contact mode, whereas they were clearly shown in the FMM image. Therefore, this case was the same as scenario A [Fig. 1(3A,4A)] and revealed that the interfacial attraction strength between GO and PVA was stronger than the interfacial forces between the graphene and mica. Thus, for GO, we concluded the following interfacial attraction strength order: PVA > Mica > PMMA > HOPG.

This result was reasonable when we considered the molecular structure of these four materials. For mica and PVA, the presence of hydroxyl groups on them allowed for the formation of hydrogen bonding between these surfaces and GO, which contained hydrogen and oxygen groups attached to the carbon backbone. Compared to mica and PVA, HOPG and PMMA were much more hydrophobic and may have been incompatible with the hydrophilic GO sheets, especially in the case of HOPG. Moreover, HOPG consisted of only pure graphite layers and

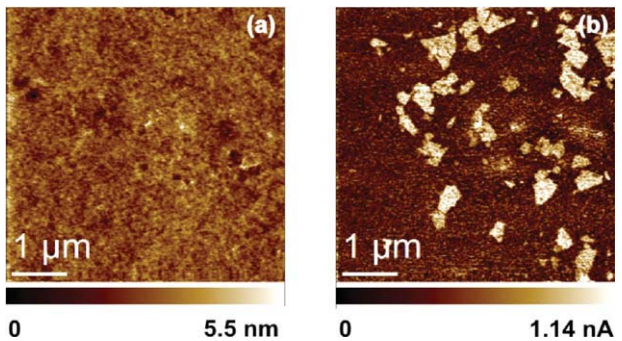

Figure 4 PVA film peeled off from the GO spin-coated mica substrate: (a) AFM topography and (b) FMM magnitude image. [Color figure can be viewed in the online issue, which is available at wileyonlinelibrary.com.]

had the planar sp^2 carbon network. The interfacial attraction between HOPG and GO may have been dominated by van der Waals forces, which are much weaker than the hydrogen bonding.

CONCLUSIONS

In this article, we developed a novel method to directly characterize and measure the relative strength of the interfacial attractive forces between GO nanoparticles and the polymer matrix on the nanoscale of an individual particle using AFM techniques. The method was successfully applied to study the interfacial attractive strength in GO–polymer nanocomposites. Two polymers, PMMA and PVA, used as matrices were studied. The results support that this method is capable of characterizing the interfacial attractive forces directly at the nanoscale of graphene with a macromolecular material. This method may be applied to other nanocomposite systems, allowing for the determination of the interaction strength between nanoparticles and the polymer. This information is paramount for achieving a fundamental scientific understanding at the molecular level of the relationship of the particle and the polymer's chemical structure to the strength of their interface. Once achieved for a variety of nanopolymer systems, this information should pave the way to understanding, predicting, and improving the composites' performance properties.

References

1. Ajayan, P. M.; Tour, J. M. Nature 2007, 447, 1066.
2. LeBaron, P. C.; Wang, Z.; Pinnavaia, T. J. Appl Clay Sci 1999, 15, 11.
3. Ramanathan, T.; Abdala, A. A.; Stankovich, S.; Dikin, D. A.; Herrera-Alonso, M.; Piner, R. D.; Adamson, D. H.; Schniepp, H. C.; Ruoff, R. S.; Nguyen, S. T.; Aksay, I. A.; Prud'homme, R. K.; Brinson, L. C. Nat Nanotechnol 2008, 3, 327.
4. Novoselov, S. K.; Geim, A. K.; Mozorov, S. V.; Jiang, D.; Zhang, Y.; Dubonos, S. V.; Grigorieva, I. V.; Firsov, A. A. Science 2004, 306, 666.
5. Novoselov, K. S.; Jiang, D.; Schedin, F.; Booth, T. J.; Khotkevich, V. V.; Morozov, S. V.; Geim, A. K. Proceed Natl Acad Sci 2005, 102, 10451.
6. Geim, A. K.; Novoselov, K. S. Nat Mater 2007, 6, 183.
7. Lee, C.; Wei, X.; Kysar, J. W.; Hone, J. Science 2008, 321, 385.
8. Gong, L.; Kinloch, I. A.; Young, R. J.; Riaz, I.; Jalil, R.; Novoselov, K. S. Adv Mater 2010, 22, 2694.
9. Paredes, J. I.; Villar-Rodil, S.; Solis-Fernandez, P.; Martinez-Alonso, A.; Tascon, J. M. D. Langmuir 2008, 24, 10560.
10. Park, S.; An, J.; Jung, I.; Piner, R. D.; An, S. J.; Li, X.; Velamakanni, A.; Ruoff, R. S. Nano Lett 2009, 9, 1593.
11. Schniepp, H. C.; Li, J. L.; McAllister, M. J.; Sai, H.; Herrera-Alonso, M.; Adamson, D. H.; Prud'homme, R. K.; Car, R.; Saville, D. A.; Aksay, I. A. J Phys Chem B 2006, 110, 8535.
12. McAllister, M. J.; Li, J. L.; Adamson, D. H.; Schniepp, H. C.; Abdala, A. A.; Liu, J.; Herrera-Alonso, M.; Milius, D. L.; Car, R.; Prud'homme, R. K.; Aksay, I. A. Chem Mater 2007, 19, 4396.
13. Schniepp, H. C.; Kudini, K. N.; Li, J.; Prud'homme, R. K.; Car, R.; Saville, D. A.; Aksay, I. A. ACS Nano 2008, 2, 2577.
14. Mkhoyan, K. A.; Contryman, A. W.; Silcox, J.; Stewart, D. A.; Eda, G.; Mattevi, C.; Miller, S.; Chhowalla, M. Nano Lett 2009, 9, 1058.
15. Stankovich, S.; Piner, R. D.; Chen, X.; Wu, N.; Nguyen, S. T.; Ruoff, R. S. J Mater Chem 2006, 16, 155.
16. Stankovich, S.; Piner, R. D.; Nguyen, S. T.; Ruoff, R. S. Carbon 2006, 44, 3342.
17. Lerf, A.; He, H.; Forster, M.; Klinowski, J. J Phys Chem B 1998, 102, 4477.
18. Kim, H.; Macosko, C. W. Macromolecules 2008, 41, 3317.
19. Kim, H.; Macosko, C. W. Polymer 2009, 50, 3797.
20. Kim, H.; Miura, Y.; Macosko, C. W. Chem Mater 2010, 22, 3441.
21. Kim, H.; Abdala, A. A.; Macosko, C. W. Macromolecules 2010, 43, 6515.
22. Cai, D.; Yusoh, K.; Song, M. Nanotechnology 2009, 20, 085712.
23. Hummers, W. S., Jr.; Offeman, R. E. J Am Chem Soc 1958, 8, 1339.
24. Radmacher, M.; Tilmann, R. W.; Gaub, H. E. Biophys J 1993, 64, 735